Plasma Phys. Control. Fusion **53** (2011) 124037 (18pp) doi:10.1088/0741-3335/53/12/124037

Plasmas for space propulsion

Eduardo Ahedo

E.T.S. Ingenieros Aeronáuticos, Universidad Politécnica de Madrid, Plaza Cardenal Cisneros, 28040 Madrid, Spain

E-mail: eduardo.ahedo@upm.es

Received 24 June 2011, in final form 6 October 2011
Published 14 November 2011
Online at stacks.iop.org/PPCF/53/124037

Abstract
Plasma thrusters are challenging the monopoly of chemical thrusters in space propulsion. The specific energy that can be deposited into a plasma beam is orders of magnitude larger than the specific chemical energy of known fuels. Plasma thrusters constitute a vast family of devices ranging from already commercial thrusters to incipient laboratory prototypes. Figures of merit in plasma propulsion are discussed. Plasma processes and conditions differ widely from one thruster to another, with the pre-eminence of magnetized, weakly collisional plasmas. Energy is imparted to the plasma via either energetic electron injection, biased electrodes or electromagnetic irradiation. Plasma acceleration can be electrothermal, electrostatic or electromagnetic. Plasma–wall interaction affects energy deposition and erosion of thruster elements, and thus is central for thruster efficiency and lifetime. Magnetic confinement and magnetic nozzles are present in several devices. Oscillations and turbulent transport are intrinsic to the performances of some thrusters. Several thrusters are selected in order to discuss these relevant plasma phenomena.

(Some figures may appear in colour only in the online journal)

1. Space propulsion

The displacement of a satellite or spacecraft in outer space and its attitude control are the task of space propulsion, which is carried out by rocket engines. These operate according to the principle of action and reaction, generating a force (or thrust) F on the spacecraft by expelling backwards a jet of gas of high kinetic energy. Chemical and electric propulsion differ in the source used to energize and accelerate the gas. Plasma propulsion uses electric energy to ionize the propellant and then impart kinetic energy to the resulting plasma. Due to several constraints, electric rockets compete with chemical thrusters only in space. Launchers, which manage enormous power and thrust, are responsible for delivering a spacecraft into space orbit. They constitute an independent technology, which is the exclusive domain of chemical rockets.

 © 2011 IOP Publishing Ltd Printed in the UK & the USA

The total propulsive workload of a space thruster is measured by ΔV, the sum of all velocity changes to be carried out on the motion of the spacecraft while traveling in near vacuum. In the proximity of large celestial bodies ΔV also includes the compensation of different ambient forces, such as gravity, atmospheric drag or radiation pressure. Orbital maintenance of geostationary communication satellites, which constitute the bulk of the spacecraft market, requires $\Delta V \sim 1\,\mathrm{km\,s^{-1}}$ for a 15-year period. ΔV of deep-space missions can be one order of magnitude larger; for instance, the Dawn mission to asteroids Vesta and Ceres, equipped with plasma rockets, has $\Delta V \sim 11\,\mathrm{km\,s^{-1}}$.

In a simple formulation, the thrust satisfies

$$F = \dot{m} c, \tag{1}$$

with $\dot{m}$ the gas mass flow and c its exhaust velocity [1]. If τ is the propulsion time (sum of all single firing times) the total impulse is $F\tau$ and the total mass of burned propellant is $M_\mathrm{p} = \dot{m}\tau$. The *specific impulse*, defined here as impulse per propellant mass unit, $F\tau/M_\mathrm{p}$, coincides with c. (It must be noted that the conventional definition of specific impulse, I_sp, is in terms of the propellant weight at the Earth's surface, $g_0 M_\mathrm{p}$, so that $I_\mathrm{sp} \equiv c/g_0$ and $c(\mathrm{m\,s^{-1}}) \simeq 10 I_\mathrm{sp}(\mathrm{s})$; our choice avoids dragging g_0 in all formulae.) The propellant mass M_p for a space mission is provided by Tsiolkovsky's equation [2]

$$\frac{M_\mathrm{p}}{M_\mathrm{f}} = \exp\frac{\Delta V}{c} - 1, \tag{2}$$

where M_f is the spacecraft mass at the mission end, sum of the payload mass and the rocket dry mass. An important part of the cost of a space mission is its launching cost, which is roughly proportional to the initial mass of the spacecraft, $M_\mathrm{f} + M_\mathrm{p}$. The exponential increase of M_p with $\Delta V/c$ in equation (2) shows how crucial it is, for ambitious propulsive missions, to select a rocket with large c. Hence, the specific impulse is the first figure of merit of a space rocket.

In a chemical rocket, the specific impulse is mainly an intrinsic characteristic of the propellant, related to its calorific energy per unit of mass, and there are natural limitations to its maximum value. The most common chemical propellant used in space is hydrazine, with a good combination of simplicity and safety in operation and storage, and a reasonable specific impulse ($c \approx 2.3\,\mathrm{km\,s^{-1}}$). In an electric rocket, the specific impulse is extrinsic and depends on the electric or electromagnetic energy deposited into the plasma, which can attain very large values. Thrusters with $c \sim 30\,\mathrm{km\,s^{-1}}$, surpassing 13 times a hydrazine thruster, are already operating commercially. The prospects of both exponentially reducing the fuel bill and making viable ambitious deep-space missions—unaffordable with chemical rockets—make plasma propulsion extremely attractive.

The second essential figure of merit of a space thruster, which assesses the efficient use of the available energy, is the *thrust efficiency*

$$\eta = \frac{F^2}{2\dot{m} P_\mathrm{a}} \equiv \frac{Fc}{2P_\mathrm{a}}, \tag{3}$$

with P_a the available (chemical or electrical) power. If the dispersion of velocities in the ejected gas is small, η is also the ratio between the jet useful power and the available power [1]. Therefore, the reduction of all sources of energy loss is essential for thruster competitiveness. An unavoidable loss in a plasma thruster is the dissociation and ionization of the embarked (neutral) gas. Therefore, propellants that minimize the specific ionization/dissociation loss are preferred from an efficiency standpoint; noble gases and alkali metals of large ion mass and low ionization energy are a good choice for propellants. Radiation losses and energy deposition at the thruster surfaces are other important losses. Thruster heating, in addition to diminishing

thrust efficiency, is a serious issue on its own, mainly for high-power propulsion, because of the difficulty of dissipating heat in space and eventual thruster malfunctioning.

The onboard electrical power available to spacecraft has so far been a heavy limitation for the development and implementation of plasma propulsion. In the near future, solar panels will continue to be the main electric energy source onboard a spacecraft. Fortunately, the installed solar array power is growing quickly, having attained already 24 kW in the largest telecom satellites. This still leaves some high-power thrusters, efficient on the megawatt-centered range, far from been flight-tested.

If P_a is limited by the power source, the available thrust is also limited. Furthermore, equation (3) indicates that for a given P_a, there is a trade-off between c and F: the larger c, the smaller is the F. This makes plasma thrusters low-thrust devices, operating on large propulsion times. Using an athletics metaphor, the chemical rocket is the 'sprinter' and the plasma rocket is the 'marathon runner', well fitted for a long propulsive journey. In fact, the Dawn mission broke the absolute record of ΔV given by any space thruster in 2010. A third relevant figure of merit is the thruster lifetime, which measures how big the total impulse can be. Among the multiple causes that eventually make the thruster non-operational, a prominent one is excessive erosion and degradation of thruster surfaces (walls, electrodes or grids).

Compared with chemical thrusters, electric thrusters and their accompanying power system are sophisticated machines, with complex power processing units and a dry mass, M_t, that can be comparable to M_p at very high c. This makes the specific mass M_t/P_a a fourth figure of merit of a plasma thruster. Indeed, for a given specific mass and propulsion time, there is an optimal specific impulse, $c_{opt} \sim \sqrt{2\eta\tau P_a/M_t}$, that minimizes the spacecraft initial-to-payload mass ratio and the mission cost [2].

Plasma thrusters constitute today a large and varied family, with nominal powers ranging from subwatt to megawatt, and specific impulses from 0.5 to 100 km s^{-1}. The ion thruster, the Hall-effect thruster, the arcjet and the pulsed plasma thruster, invented 50 years ago, constitute the group of devices already commercialized by space companies. In recent years, the excellent perspectives of plasma propulsion have boosted the development of other prototypes and the invention of new ones, sometimes based on devices from other plasma applications (such as fusion or material processing).

Plasma thrusters can be classified according to the mechanisms for plasma production and plasma acceleration. Plasma production and heating is achieved by either direct-current (dc) biased electrodes or alternate current (ac) antennas, radiating mainly in the radiofrequency (RF) or microwave ranges. The dc biased electrodes are used in most veteran designs, but suffer from electrode erosion. The ac-based devices must care about electromagnetic interferences and inefficiencies in the wave energy conversion and transmission.

Plasma acceleration mechanisms are best identified in the momentum equation of a fully ionized plasma,

$$\nabla \cdot \rho \boldsymbol{u}\boldsymbol{u} = \epsilon_0(\nabla \cdot \boldsymbol{E})\boldsymbol{E} + \boldsymbol{j} \times \boldsymbol{B} - \nabla \cdot \bar{\bar{P}}. \tag{4}$$

Here, ρ is the mass density, $\boldsymbol{u}$ is the fluid velocity of the plasma, $\boldsymbol{j}$ is the electric current density, $\bar{\bar{P}}$ is the pressure tensor (with partial contributions of ions and electrons), ϵ_0 is the vacuum permittivity, and $\boldsymbol{E}$ and $\boldsymbol{B}$ are the electric and magnetic fields, which can be either applied externally or self-induced by the plasma. Both ρ and $\boldsymbol{u}$ are determined by the massive ions, while the main contribution to $\boldsymbol{j}$ comes generally from electrons. The pre-eminence of any of the three terms on the right-hand side of equation (4) classifies a plasma device as *electrostatic*, *electromagnetic* or *electrothermal* accelerator [3]. The main component of thrust comes from the integration of the axial component of the plasma momentum flux in

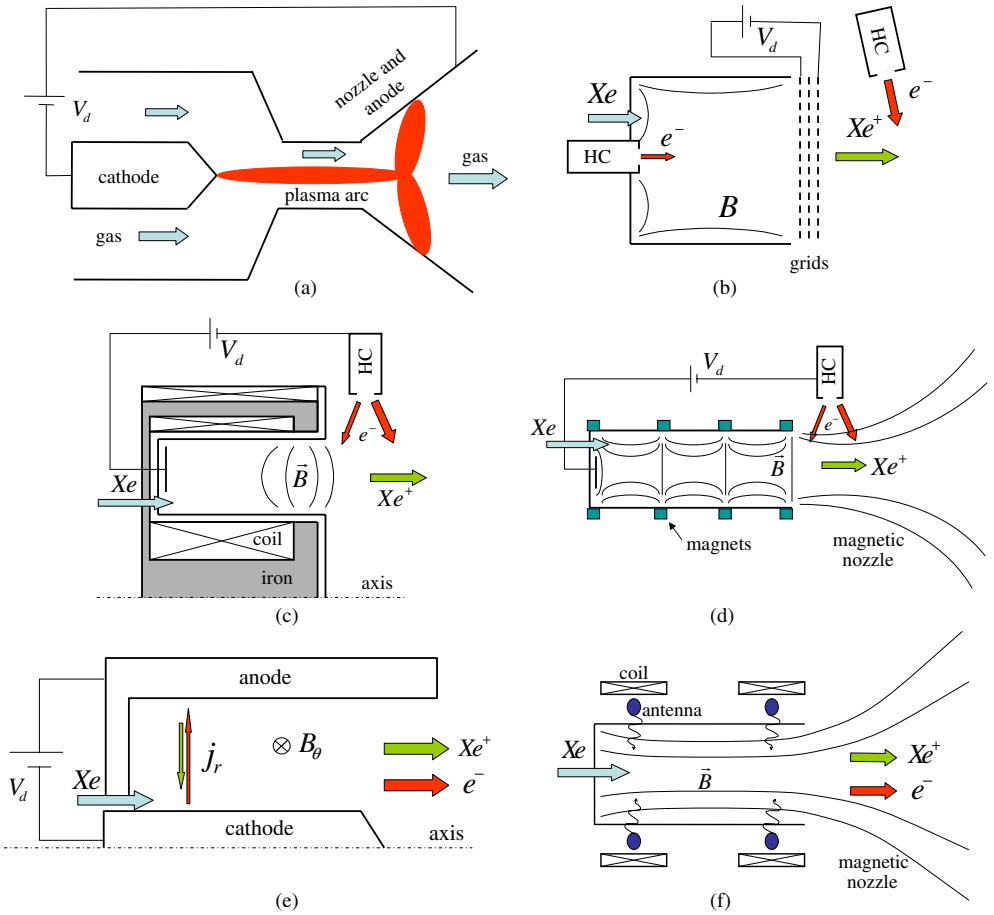

Figure 1. Schematic of several plasma thrusters: (*a*) arcjet, (*b*) dc ion thruster, (*c*) Hall effect thruster, (*d*) Hall effect thruster with magnetic cusps, (*e*) magnetoplasmadynamic thruster, (*f*) helicon thruster. HC means hollow cathode and xenon is assumed as propellant.

equation (4) over a plane perpendicular to the beam and located far downstream, where the thruster electromagnetic field has vanished.

A classical representative of electrothermal thrusters is the arcjet, figure 1(*a*), which is basically a chemical thruster where gas is super-heated by a plasma arc. The arc is formed between a central rod, acting as the cathode, on the upstream side of the thruster nozzle and the anode located in the divergent nozzle wall. The arc is stabilized with a constricted channel at the nozzle throat. Most of the mass flow remains in the neutral gas, which surrounds the low-density plasma arc. A strong radial gradient of temperature keeps temperatures of ∼20000 K at the arc and ∼2000 K at the gas near the walls. The thermodynamics of this device reside mainly in the domain of chemical rockets. A hydrazine arcjet reaches a specific impulse of $c \sim 6\,\mathrm{km\,s^{-1}}$, instead of the $2.3\,\mathrm{km\,s^{-1}}$ of an only-chemical hydrazine thruster. Electrode erosion limits the lifetime of the arcjet to ∼1000 h.

Genuine plasma thrusters ionize nearly all the gas injected in them. Typical ranges of plasma densities and temperatures are $n_\mathrm{e} \sim 10^{17}$–$10^{20}\,\mathrm{m^3}$ and $T_\mathrm{e} \sim$ 2–40 eV. The Debye length is generally the smallest length scale of the problem ($\lambda_\mathrm{d} \sim$ 1–100 μm), so that the

plasma is quasineutral except in thin Debye layers around the chamber walls, electrodes and grids; the resulting ambipolar electric field in the quasineutral plasma makes the electrostatic term of equation (4) negligible. Frequently the plasma is weakly collisional too, which favors magnetic confinement, if needed, but keeps the plasma off local thermodynamic equilibrium, with the resulting uncertainties on the species velocity distribution function (VDF) and the plasma transport coefficients.

In the rest of this paper we will comment on the relevant plasma phenomena taking place in space thrusters, with special mention of some open problems. Two mature and two laboratory-level plasma thrusters will be used for this presentation. Thus, this paper does not attempt to provide a complete overview of plasma physics in space propulsion, which exceeds clearly the frame of this article and likely the skills of its author. For a broader perspective, the reader is referred to the textbook by Jahn [3], the open course by Martínez-Sánchez [4] and their succinct overviews [5, 6]. Overviews of different plasma thrusters are collected in *Journal of Propulsion and Power* (vol 14, no 5, 1998) and the *Encyclopedia of Aerospace Engineering* (chapter 'Alternative Propulsion', Wiley Online Library, 2010) and recent advances in the field are presented in a special issue of *IEEE Transactions of Plasma Science* (vol 36, issue 5, part 1, 2008).

2. The ion thruster

This veteran thruster and the best example of electrostatic acceleration is basically a modified ion source, a device with multiple applications [7]. It consists of a plasma generation chamber and a set of, at least, two grids, see figure 1(*b*). These extract the ions from the chamber and accelerate them to energies of ∼1–2 kV [8, 9]. Conversely, the electric reaction force of ions on the grids constitute the thrust. Simultaneously, the grids act as a barrier for electron crossing in both directions. In some concepts, a third grid is added on the outside to screen backscattered ions. An external hollow cathode provides the electron current that makes the expelled beam quasineutral and net-current free.

The grid system is a critical element of an ion thruster (IT). First, grid transparency and alignment must satisfy conflicting requirements of maximizing the extracted current, minimizing ion impact on the grids, keeping structural integrity and delivering a low-divergence ion beam. Second, the ion current density, j_i, extracted from the chamber is upper-bounded by space-charge saturation at the grids: the maximum j_i satisfies Child's law

$$(j_\mathrm{i})_\mathrm{max} = \frac{4\epsilon_0}{9}\left(\frac{2e}{m_\mathrm{i}}\right)^{1/2}\frac{V^{3/2}}{d^2}, \tag{5}$$

where d and V are the inter-grid distance and voltage. The grid separation is of the order of 1 mm, which constitutes a structural, electrical and thermal challenge. The electrical or structural failure of highly eroded grids is the main lifetime limitation of this thruster. Nonetheless, the IT bears the longest lifetime among plasma thrusters, approaching 30 000 h in recent designs. The dependence $j_\mathrm{i} \propto V^{3/2}$ explains that the IT is a high-voltage, low-current and bulky device. The management of high voltages and powers in space and the control of the multiple electrical points of the system are the other challenging aspects of these devices and the reason for their sophisticated and heavy power processing unit.

Using Child's law and $c \sim \sqrt{eV/m_\mathrm{i}}$ for the specific impulse, the thrust density (per unit of frontal area A) scales as

$$F/A \propto c^4 m_\mathrm{i}^2/d^2. \tag{6}$$

Taking the optimal specific impulse for a given mission heavy ions allows a higher thrust density (at a higher voltage) and thus a more compact device. Current ITs operate mostly

with xenon (which in addition, is chemically inert and easy to manage) and typical specific impulses of 25–40 km s^{-1}.

IT types differ by the ionization mechanism they implement. In the classical dc IT a second hollow cathode, placed in the chamber, injects primary electrons of 10–30 eV to drive ionization. The bulk of the electron density is a cloud of secondary electrons of 2–5 eV, product of ionization. Near-total propellant ionization requires good confinement of primary electrons, which is achieved by a system of coils or magnets that configure a magnetic field mostly parallel to the chamber walls. Modern designs tend to use cusped-field configurations that maximize magnetic confinement.

The second type of ITs replace the internal hollow cathode by a RF or microwave antenna, generally located outside the plasma chamber. In a RF IT the emitted wave is coupled to the plasma inductively, so that electron heating takes place in a region of the order of the electron skin depth around the chamber boundary. The RF IT has been researched for 40 years and has been space-tested [10]. Thrust efficiency is a bit smaller than in the dc IT, but bears several attractive features: magnetic confinement is not required, plasma potentials in the chamber are smaller than in the dc engine—thus reducing internal erosion, the electrical control is simpler and RF waves do not present electromagnetic interferences in the spacecraft environment.

The electron-cyclotron-resonance (ECR) IT is a less developed device, but has already been flown, propelling the Hayabusa mission [11]. Strong magnet rings ($\sim$0.3 T) and a 2.4 GHz wave emission create an ECR layer (in the region with 0.15 T). Careful design was required in order that the microwave was not reflected back before reaching the ECR layer. This implied a low plasma density away from the ECR annular layer, which had a heavy toll on thrust efficiency. Electromagnetic interferences with communication lines are also an issue when using microwaves.

Electrostatic acceleration of charged ions or droplets extracted from fine needles by kilovolt-biased electrodes are the basis of *electrospray micro-propulsion* [12]. Tens to thousands of individual emitters are arranged in arrays or slits for versatile operation and provide thrust in the range $\sim$1–10^3 μN. This technology, practically abandoned in the 1970s, was revived 20 years ago, thanks to the advances made on electrosprays for industrial applications and microfabrication. It is considered a very attractive option for the high precision and thrust controllability requirements of some scientific missions. Electrospray propulsion includes colloidal thrusters, field emission electric propulsion (FEEP) devices [13], and ionic liquid ion source (ILIS) devices. The two first concepts will be flight-tested in the coming LISA Pathfinder mission, while the last one, with some promising advantages [12], is still at the laboratory stage.

3. The Hall-effect thruster

The Hall-effect thruster (HET), figure 1(*c*), is a direct competitor of the IT and is also widely commercialized. The conventional design of a HET consists of an annular, dielectric chamber with the gas injection and a metallic anode at its back [14, 15]. An external hollow cathode acts as the cathode and sole source of electrons. Except in (non-neutral) sheaths around the walls the plasma is quasineutral and the self-adjusted ambipolar electric field governs ion and electron dynamics. The electron current emitted by the hollow cathode is the discharge current I_d on the external circuit and is self-split into two beams. One beam (carrying about 60–80% of I_d) travels downstream and neutralizes the ion beam ejected from the chamber. The second electron beam travels inward; it is first energized by Joule heating and then initiates the ionization of the neutral gas in the chamber. New born electrons help to complete ionization.

Ions are extracted and accelerated by the electric field between their birth place and the external cathode region. Once outside, the ion beam joins the second beam of electrons from the hollow cathode, as in an IT.

In order to have an adequate plasma density ($n_e \sim 10^{17}$–$10^{18}\,\mathrm{m}^{-3}$) and near-total gas ionization, the axial electron flow is strongly inhibited by applying a near-radial magnetic field of a few hundred Gauss. This is generated by a magnetic circuit consisting of an iron core structure and several coils around the plasma chamber. The magnetic field induces $E \times B$ and diamagnetic azimuthal drifts on the electrons, which constitute the Hall current that gives the name to the device. In addition, it inhibits electron perpendicular transport, making it rely on collisional and turbulent transport. The magnetic field is too weak to directly affect the ion motion, but it shapes the electric potential map, since equipotential lines try to be aligned with magnetic lines. Hence, HET performance is quite sensitive to the magnetic field topology.

According to equation (4), the HET is an electromagnetic plasma accelerator, where the plasma momentum gain comes mainly from the magnetic force due to $j_\theta B_r$ [3]. The thrust, exerted by the plasma on the thruster structure, also has an electromagnetic nature: it consists of the reaction force constituted by the magnetic field induced by the plasma Hall current on the coil current (the effect on the induced magnetic field on the plasma itself is negligible). While the plasma as a whole is accelerated electromagnetically, the unmagnetized ions are accelerated electrostatically by the ambipolar electric field. This field does not appear in the *plasma* equation (4), but it amounts to most of the term $\boldsymbol{j} \times \boldsymbol{B}$. This behavior is common to most thrusters operating with quasineutral plasmas.

A commercial HET operates typically with xenon and a discharge voltage V_d of about 200–400 V. This yields a specific impulse of 15–20 $\mathrm{km\,s}^{-1}$, which is optimal for in-orbit maintenance of geostationary satellites. The lower voltages, the smaller number of electric points to control and the larger ion current density, make the HET simpler electrically and more compact than the IT. The ion current of a HET is proportional to $\dot{m}$ and is independent of V_d. This yields a sizeable throttling capability to the HET, which augments its span of possible missions. Indeed, modern HET designs tend to be dual mode, in order to operate at either 'high' thrust (e.g. for orbit insertion) or high specific impulse (e.g. for orbit stationkeeping).

On the negative side, a HET, compared with an IT of a similar power, has a lower thrust efficiency (50–55% instead of 65–70%), about half the lifetime and a larger plume divergence. This last feature can be a serious concern, because of the potential damage of very-energetic particles impacting sensitive spacecraft parts, such as a large solar panel. The large (peak) temperature of a HET plasma ($T_e \sim 20$–40 eV, typically) is at the core of negative effects that reduce the thrust efficiency: the large plume divergence, the generation of doubly charged ions (which have a higher ionization cost per unit of charge), and high energy losses at the chamber walls.

Fluid-like [16–18] and particle-based [19–24] models and codes have been successful in explaining the complex interplay of processes and parameters in a HET discharge. However, there are two groups of important plasma processes that are still far from being satisfactorily mastered. These are plasma–wall interaction phenomena, and axial electron transport and related instabilities.

3.1. Plasma–wall interaction phenomena

Plasma–wall interaction in a HET is determined by the magnetic field topology, the wall material, and the VDF of ions and electrons. First, there is no magnetic confinement of the HET lateral walls: magnetic lines are near perpendicular to them, and plasma fluxes there produce significant recombination and energy deposition. Second, in order to have a gentle

potential fall between anode and external cathode, the chamber of a conventional HET is fabricated of dielectric material, generally a boron nitride and silica compound (BN–SiO_2), which features a good combination of electrical, thermal and mechanical properties. But dielectric materials present large secondary electron emission (SEE) by electron impact. The secondary-to-primary electron flux ratio, known as the SEE yield, δ_s, surpasses 1 for electron energies of 30–50 eV. The exchange of hot electrons from the plasma by cold electrons from the wall implies large energy losses.

Taking into account the flux of secondary electrons, the zero-current balance at the dielectric wall is $|j_i| = |j_e|(1 - \delta_s)$. Here, the ion current density j_i is fixed by the Bohm condition at the sheath edge [25, 26], whereas the current density of primary electrons j_e is related to the potential fall at the sheath, ϕ_{sh}, by $|j_e| \propto \exp(-e\phi_{sh}/T_e)$. Thus, the zero-current condition determines ϕ_{sh}, which decreases with increasing δ_s. For a near-Maxwellian electron VDF there is charge saturation at the wall-sheath interface when $\delta_s \simeq 0.98$. This acts as an upper barrier for the effective SEE flux that crosses the sheath (similar to the Child's law effect in ITs), and the sheath does not vanish [27]. However, from $\delta_s = 0$ to $\delta_s \sim 0.98$, the relative potential fall, $e\phi_{sh}/T_e$, decreases from $\sim$5 to $\sim$1, and both $|j_e|$ and the energy deposition at the wall ($\simeq 2T_e|j_e|$) increase by two orders of magnitude [28].

In practice, energy losses at the walls are surely lower since electron collisionality is relatively weak in a HET and the tail of energetic electrons that are collected by the walls is likely to be highly depleted [29, 30]. This would significantly reduce the electron current j_e to the wall, but reliable models for a non-Maxwellian VDF are lacking. Further uncertainties are related to the evolution within the bulk of the plasma of the SEE beams from the two lateral walls. If their thermalization time is large, they could remain as distinguished populations, affected by magnetic mirror effects, and they could be recollected back by the walls [31]. Alternatively, the two-stream instability could accelerate their thermalization [30].

HET lifetime is limited by large erosion of the chamber walls by ion sputtering. Because of the mild electrostatic confinement at the walls, the ion flux to the wall is relatively large; indeed, it amounts typically to 30–40% of the total ion production [14]. Ions accelerated radially by presheath and sheath potential fall, impact the walls with considerable energy and then recombine. Erosion of the dielectric material leads first to a widening of the channel—thus modifying plasma/thruster performance—and eventually to thruster failure, because of deficient thermal and electrical insulation. The possibility of conducting reliable simulations of chamber erosion would be very beneficial to reduce long and expensive life tests of a HET in vacuum chambers (of course, the same is true for other plasma thrusters). Those simulations require to know both the VDF of heavy species and the sputtering yield function of the wall material in terms of energy and angle at impact [32]. At present, plasma simulations are not predictive and the sputtering yield is poorly known. Sputtering of compound ceramics depends on many aspects (such as the compound percentage, grain size and orientation, and the differential sputtering of each component) and is difficult to reproduce even in semi-phenomenological formulations. In addition, experimental characterization of the sputtering yield is delicate, mainly below 100 eV—a range of interest inside the HET chamber, where sputtering is small and thus subject to measurement errors [33]. Abnormal erosion in the form of striations has also been observed, likely connected to details of the electron VDF [34].

3.2. Perpendicular electron transport and instabilities

From the pioneering times of HET research it was realized that electron transport perpendicular to the magnetic field was much larger than that expected from classical collisionality [35, 36]. This anomalous diffusion was postulated to be due to either wall collisionality (also called

near-wall conductivity [37]) or turbulent transport. Wall collisionality would consist of the exchange of magnetized primary electrons by unmagnetized secondary electrons: as in a classical collision of an electron with a heavy particle, the after-collision electron advances on the average one Larmor radius before it is trapped in a magnetic field line. In a macroscopic electron model, wall collisionality appears as a contribution to the azimuthal momentum equation. Recent evaluations of wall collisionality [16, 38] suggest that it is insufficient to explain the electron anomalous diffusion, which leaves turbulent diffusion as the main candidate.

Many plasma oscillation modes have been identified in a HET, propagating either azimuthally or longitudinally, ranging from a few kHz to tens of MHz [39]. Some relevant longitudinal and low-frequency modes are reasonably well understood. This is the case of the ion-transit mode in the range 100–500 kHz [40] and the breathing mode in the range 10–30 kHz [41]. This last one involves the interaction of standing plasma waves with standing and convective neutral waves and is responsible for large oscillations of I_d, that must be limited by appropriate filters in the external electric circuit. In contrast the state of knowledge of azimuthal modes is poorer, partly because there are few analyses with discharge models that include azimuthal gradients.

Turbulent electron diffusion would be due to correlated azimuthal fluctuations of plasma magnitudes (mainly density and electric field) that would leave a time-averaged azimuthal force on electrons, F_turb. The essence of this force is disputed but its effect on the plasma would be simple to interpret. In a time-averaged axisymmetric configuration the electron perpendicular velocity (in the meridian plane) $u_{\perp e}$ satisfies

$$m_\mathrm{e} n_\mathrm{e} u_{\perp e} \simeq \frac{\nu_\mathrm{e} F_\perp + \omega_\mathrm{ce} F_\mathrm{turb}}{\omega_\mathrm{ce}^2}, \tag{7}$$

with $F_\perp$ the perpendicular (electric plus pressure) stationary force, ω_ce the electron cyclotron frequency and ν_e the classical-plus-wall collisionality frequency. Since the Hall parameter $\chi = \omega_\mathrm{ce}/\nu_\mathrm{e}$ is about 10^3, it suffices a very small turbulent force, namely $\alpha_\mathrm{turb} \equiv F_\mathrm{turb}/F_\perp > \chi^{-1}$ for the perpendicular electron diffusion to be dominated by the turbulent force instead of by classical collisionality. Measurements of perpendicular diffusion suggest an average turbulence level of $\alpha_\mathrm{turb} \sim$ 1–5%, which means that perpendicular diffusion is mainly a collisionless, turbulent process. This was first suggested by Janes and Lowder [35], who attributed the turbulent force to an azimuthally rotating spoke of ∼25 kHz; a similar spoke has been observed recently [42]. Other authors claim that F_turb comes, at least partially, from the observed fluctuations in the range of several MHz [43]. Attempts to determine whether turbulent diffusion is larger inside the chamber or in the near plume (where plasma conditions are not the same) have not been very conclusive. Therefore, turbulent diffusion in HETs is a problem far from being solved. Much experimental and theoretical work is ahead, and this could benefit from the existing knowledge in the plasma fusion field [44].

3.3. Alternative designs

There exist several variants of the conventional HET offering improved solutions to different aspects of a conventional HET. The thruster with anode layer or *TAL-type HET* is a HET with a short, metallic chamber and is operational too [15]. The low SEE yield of metals implies a much lower energy deposition at the walls, but this gain seems to be compensated by less efficient ionization and acceleration processes, since thrust efficiencies are similar.

The thrust efficiency of a conventional HET design deteriorates below 200–400 W. Dimensional analysis indicates that magnetic field and plasma density should scale inversely proportional to the discharge power [45, 46], but this leads to higher thermal loads and energy

losses, shorter lifetimes and severe technological challenges. Two alternatives have been proposed. First, the *cylindrical HET* which tries to remedy this by eliminating partially or totally the central rod and re-shaping partially the magnetic topology [47]. Second, the *mini-HET with permanent magnets*, which can keep large magnetic fields without spending power in the magnetic circuit, at the cost of very limited throttling [48].

The *two-stage HET* introduces an intermediate electrode, which can be electron emissive or not, with the idea of better controlling the plasma discharge and thus to enhance efficiency [49]. Although this enhancement has been proven theoretically, practical prototypes have been unsuccessful so far, due to both technical difficulties and insufficient comprehension of the two-stage discharge [50, 51].

The weakest aspect of a conventional HET is the lack of magnetic confinement at the chamber lateral walls. The very recent *HET with magnetic cusps,* figure 1(*d*), known with the abbreviations HEMP in Germany [52] and DCFT in the USA [53], attempts to solve this with an innovative magnetic topology. The device consists of a cylindrical or conical chamber with a set of alternate ringed magnets. These create a cusped magnetic configuration that magnetically screens most of the wall surface, thus drastically diminishing the plasma fluxes to the wall [54], and the associated energy deposition and ion sputtering. At the same time, the magnetic lines emanating from the cusp centers are near-radial and provide the axial magnetic barrier that inhibits electron transport. Tests with a first 250 W-prototype have shown that its thrust efficiency can compete with flight-qualified HETs in the same range [53]. The propellant ionization seems rather modest (say 70%) but this is more than compensated by the low energy deposition at the walls. The detailed plasma behavior inside the chamber is still largely unknown.

4. The magnetoplasmadynamic thruster

The magnetoplasmadynamic thruster (MPDT), figure 1(*e*), consists of an annular chamber with a central cathode and an anode ring, biased to a discharge voltage V_d, typically in the range 50–300 V [3, 55, 56]. Usually, the shape of the anode ring is slightly divergent, in order to provide a nozzle effect on plasma acceleration (and reduce the energy dissipation there). The propellant is injected at the back of the chamber and becomes ionized by electron impact. The resulting plasma maintains the discharge current I_d between electrodes. The magnetic field in the MPDT, B_θ, is azimuthal and self-induced by the longitudinal plasma current density $\boldsymbol{j}$. The integration of Ampere's law, $\nabla \times \boldsymbol{B} = \mu_0 \boldsymbol{j}$, yields that the magnetic field is maximum at the chamber back-plate, amounting there to $B_\theta(r) \sim \mu_0 I_\mathrm{d}/(2\pi r)$. Plasma density in a MPDT is $n_\mathrm{e} \sim 10^{20}$–$10^{21}\ \mathrm{m}^{-3}$, larger than in an IT or a HET, whereas T_e is below 10 eV.

Contrary to a HET, the plasma flow along the MPDT chamber is net-current free and no external neutralizer is required. Plasma axial acceleration, equation (4), is due to the combined effects of the thermal pressure gradient and the Lorentz force, and this one consists mainly of the gradient of the magnetic pressure $B_\theta^2/(2\mu_0)$. Therefore, the plasma parameter β, ratio between the thermal and magnetic pressures, determines the operation regime of a MPDT. Since $B_\theta \propto I_\mathrm{d}$, the magnetic pressure is small at low I_d, and the MPDT acts as an electrothermal device. This is a very inefficient operational regime because of poor propellant ionization and large electrode losses. At high enough I_d, the magnetic pressure dominates and the MPDT operates properly as an electromagnetic device. The transition between both regimes is observed clearly in experimental data as a change of slope in the current-voltage curves (from $V_\mathrm{d} \propto I_\mathrm{d}$ to $V_\mathrm{d} \propto I_\mathrm{d}^3$).

The requirement of high discharge current makes the MPDT a high-power device only. For instance, taking $n_\mathrm{e} = 10^{21}\ \mathrm{m}^{-3}$ and $T_\mathrm{e} = 3\,\mathrm{eV}$, the transition $\beta = 1$ takes place at

$B_\theta \simeq 350\,\mathrm{G}$, which, for an average chamber radius of 3 cm, requires $I_\mathrm{d} \simeq 5200\,\mathrm{A}$ and thus a power of ∼0.5 MW. In the electromagnetic regime, the integration of the Lorentz force over the discharge volume yields that the thrust scales as [5] $F \sim \mu_0 I_\mathrm{d}^2/4\pi$; the same quadratic dependence on I_d is followed by the specific impulse.

In addition to β, the two-dimensional behavior of the plasma flow in the MPDT channel is characterized by two other parameters: the magnetic Reynolds number, Rm (based on the exhaust velocity, say), and the Hall parameter, χ. In the electromagnetic regime, Rm tends to be large (with $Rm \propto \beta^{-1}$) and the plasma flow is MHD-like. For $Rm \gg 1$, the back electromotive force, caused by the axial plasma motion, cancels most of the driving radial electric field, and the plasma current between electrodes tends to concentrate in a thin layer of thickness $\sim L/Rm$, with L the channel axial length [57]. This means an increase in the current density $\propto I_\mathrm{d}^3$ and a quick increase in electrode erosion. In addition, the attachment of the plasma to the anode weakens, because the ion-attracting potential of the anode sheath decreases in order to accommodate the larger current density.

In the electromagnetic regime, the Hall parameter of a MPDT is generally $O(1)$ (it is equal to 1.4 for the example in the paragraph above and $\beta = 1$). Were the Hall parameter small the inter-electrode plasma current $\boldsymbol{j}$ would be near radial. For $\chi = O(1)$, the Hall effect provides a significant axial component to the plasma current layer, which then tends to attach at the upstream base of the cathode and the downstream lip of the anode. The Hall effect also pinches the plasma away from the anode, thus worsening the attachment there. Since most of the plasma current density is driven by electrons, the axial Lorentz force in equation (4) comes mainly from an ambipolar electric field; therefore, ion acceleration is basically electrostatic in the MPDT too.

The steady-state operation of an MPDT is upper-bounded in power by the *onset phenomenon*. This is characterized by the onset of strong voltage oscillations, followed by very large electrode erosion, mainly at the anode lips. Different theories (often complementary) have attempted to explain it [56]. A central one is based on *anode starvation*, which would start when the current density at the anode reaches the value of the thermal current density, $j = en_\mathrm{e}\sqrt{T_\mathrm{e}/(2\pi m_\mathrm{e})}$. Then the anode sheath vanishes, ions cannot be driven to the anode vicinity anymore, and the plasma detaches from the anode [58]. A vacuum arc would develop there, which would lead to visible material evaporation from the anode. (Interestingly, anode sheath vanishing has also been identified as the onset of an unstable operation case in HETs [15, 59].) A second theory relates the onset phenomenon to full ionization: once this is achieved, the surplus of energy transmitted to the plasma arc between electrodes would heat it, leading to its unstable filamentation [4]. A third category of onset theories groups a variety of plasma instabilities, but conclusions are not well established [56].

Although the MPDT was conceived more than 50 years ago, its full maturation has been hampered by a variety of shortcomings. First, the electrode erosion (in the nominal electromagnetic and non-oscillatory regime) is large, limiting the lifetime below 1000 h. Second, its thrust efficiency is modest (below 40%) because of the high power losses at the electrode sheaths and the high ionization cost (increased by large ion recombination at the cathode). Recent developments using lithium (with 5.4 eV as first-ionization energy, compared with 15.8 eV for argon) as propellant and multichannel hollow cathodes promise to solve the cathode erosion problem while raising the thrust efficiency at moderately high power levels [56, 60]. Finally, the high-power requirement has heavily hindered both the much needed vacuum-chamber tests and the collection of research funds to a technology with no flight demonstration in the foreseeable future. Quasisteady pulsed operation could be a possible escape solution, but it drags the complexity of the electrical power processing unit [61]. Nonetheless, if megawatt sources became available in space, the MPDT would keep

the unique capability of processing very high power levels in a simple, compact and robust device producing thrust densities as high as $10^5\,\mathrm{N\,m^{-2}}$, compared with $10^2\,\mathrm{N\,m^{-2}}$ in a HET and still lower values in an IT.

The *applied-field (AF) MPDT* consists of a MPDT chamber plus a set of coils that create a longitudinal magnetic field [62]. This field induces an azimuthal (i.e. Hall) current in the plasma, so that the resulting axial Lorentz force, $j_r B_\theta - j_\theta B_r$, adds to the contributions of the self-field B_θ, the radial AF B_r. Prototypes have been built in 'high' (>100 kW) and 'mid' (<30 kW) power ranges [60]. In the high-power range, the AFMPDT would attempt to make a self-field MPDT more efficient. In the low-power range, the self-field is fully negligible and the AFMPDT should be considered as an independent thruster type, with the annular chamber as the plasma production stage and the magnetic nozzle, shaped by the applied magnetic field, as the acceleration stage (magnetic nozzles are commented in the next section). The *MPD arcjet* [63], an arcjet with an applied magnetic field, can be included within the mid-power AFMPDT group. The study of the high-power AFMPDT is quite challenging: the self- and applied magnetic fields make the ion and electron flows three dimensional; and the AF is likely to inhibit largely the radial inter-electrode current.

Other electromagnetic accelerators relying on the induced magnetic field are the speculative, high-power *pulsed inductive thruster (PIT)* [64] and the mature, low-power *pulsed plasma thruster (PPT)* [65]. The PPT operates by creating a pulsed, high-current discharge across the exposed surface of a solid propellant. The arc discharge ablates and ionizes material from that surface, and then accelerates the plasma thanks to the induced magnetic field. Typical specific impulses range from 3 to 50 $\mathrm{km\,s^{-1}}$. The PPT is a compact and flexible device with a long flight record. Its simplicity makes up for its rather low efficiency (∼10%) and large specific mass.

5. The helicon thruster

Helicon sources have numerous industrial applications since they produce higher density plasmas than other RF sources at the same power level [66]. The helicon thruster (HelT) is basically a modified helicon source. The few prototypes being built so far of this newcomer [67–71] are trying to assess the range of its propulsive capabilities. The HelT is a good example of promising advanced plasma propulsion, featuring efficient RF energy deposition to produce a hot plasma and a magnetic nozzle to accelerate it.

The thruster, figure 1(*f*), consists of a dielectric tube (made of quartz normally), surrounded by coils, which generate a magnetic field of several hundred Gauss and a RF antenna, emitting in the range 1–25 MHz. Inside the tube, the applied magnetic field B is quasi-axial and has the primary function of making the plasma transparent to the propagation and absorption of helicon waves, and the secondary function of confining the plasma away from the tube lateral wall. Outside the tube, the divergent magnetic lines diverge, constituting a magnetic nozzle that guides the plasma beam.

The typical operation range of an helicon source is [72] $\omega_{lh} \ll \omega \ll \omega_{ce} \ll \omega_{pe}$, with ω_{lh} the lower-hybrid frequency, ω the wave frequency, $\omega_{ce} \propto B$ the electron cyclotron frequency and $\omega_{pe} \propto n_e^{1/2}$ the plasma frequency. Helicon waves pertain to the branch of whistler waves; in a cold, unbounded plasma, no other waves can propagate in that frequency range [73]. The basic dispersion relation for a uniform plasma and magnetic field shows, first, that there is a resonance at $\omega = \omega_{ce}\cos\theta$, with θ the angle between the wavenumber vector and the magnetic field. Second, for a given B there is a finite range of n_e—usually called the blue regime—where the helicon waves propagate. Third, these waves couple with short-wavelength,

dissipative Trievelpiece–Gould (TG) waves, which transmit the wave energy to the plasma [74, 75]. Outside the blue regime there is just an inductive plasma–wave coupling (as in the RF IT).

Part of the wave energy deposited in electrons is spent in ionizing the propellant and the rest is converted in the magnetic nozzle into directed kinetic energy of ions [76]. From this point of view, the HelT is an electrothermal accelerator and a high T_e (of several tens of eV) is needed in order to achieve attractive values of specific impulse and thrust efficiency. This requirement distinguishes the HelT from an industrial helicon source which operates typically with $T_e \sim 3$–5 eV.

In fact, the existing knowledge on the electron heating process is rather limited. First, most studies deal with wave absorption in a 1D cold plasma column, confined in a closed cylindrical resonator (with strong wave reflections at the two tube ends). Few studies address the real case of a longitudinally nonuniform plasma flowing out of the tube [77]. Second, several experiments (but not all) have detected a two-temperature population of electrons from the helicon source [78–80]. However, the conditions favorable for the generation of highly energetic electrons and the resulting form of the electron VDF remain to be clarified. This seems crucial since a two-temperature electron VDF may significantly affect plasma ionization and its subsequent expansion. For instance, it is known that such a type of VDF leads to the steepening of the plasma axial profile or, in a limit case, the formation of a non-neutral double layer within the plasma jet [81–84]. Since ions are accelerated across the potential fall of that double layer, it was suggested this could be the basis of an enhanced type of plasma thruster, referred to later as the helicon double layer thruster [85]. However, no thrust contribution can be expected from a double layer, since it just transforms electron momentum into ion momentum, while keeping the total plasma momentum constant [86–88].

Inside the cylindrical source, the plasma is magnetized and the applied magnetic field helps in generating an electron azimuthal current $j_{\theta e}$ (and a much smaller ion azimuthal current). That current is diamagnetic and provides the radial magnetic force that balances the pressure gradient,

$$0 \simeq -\partial(T_e n_e)/\partial r + j_{\theta e} B_z, \tag{8}$$

except near the tube walls where inertia effects and the electric force become dominant [89]. This magnetic confinement, which is indeed a θ-pinch [90], can reduce n_e by two orders of magnitude from the axis to the wall [91]. Both the diamagnetic current and plasma collimation (caused by the strong confinement) are crucial for an efficient expansion of the plasma beam in the magnetic nozzle.

5.1. Magnetic nozzles

For the HelT to be efficient, it is necessary that the plasma, at the exit of the source, be fully ionized and hot (and thus weakly collisional). For typical magnetic fields ($\sim$0.1 T) and propellants electrons are strongly magnetized, but ions are weakly magnetized. Thus, in the zero electron Larmor-radius limit, electron streamlines lie on the surfaces of the divergent magnetic streamtubes. Since weakly magnetized, massive ions tend to diverge less than electrons, a strong ambipolar electric field, perpendicular to the magnetic lines, develops in order to keep quasi-neutrality. This field bends the ion trajectories outward, while largely increasing the radial rarefaction of the plasma plume. [92].

The name 'magnetic nozzle' is justified because of the essential similarities between the axial expansion of the plasma in it and of a hot gas in a solid nozzle: first, there is the conversion of internal energy (of electrons) into directed axial energy (of ions), with the intermediation here

of the ambipolar electric field; second, there is an increment of the gas axial momentum flux (and therefore a thrust gain) due to the increase in the nozzle area. Beyond these resemblances in the axial response, there are significant differences. In the plasma/magnetic nozzle case, radial rarefaction is larger, azimuthal flows develop, and the thrust transmission mechanism is different [92]. In a solid nozzle, thrust is achieved by the axial component of the gas pressure on the divergent nozzle walls. In a magnetic nozzle, thrust comes from the magnetic force exerted by the Hall current on the thruster coils. This is the reaction to the magnetic force, $-j_{\theta e}B_r$ in equation (4), of the coil currents on the plasma. Therefore the magnetic nozzle constitutes an electromagnetic accelerator (but again ions are accelerated mainly by the electrostatic field).

There is no paradox in the double electrostatic/electromagnetic character of a HelT since $j_{\theta e}$ has indeed an electrothermal origin: equation (8) shows that the azimuthal current formed inside the source is proportional to the electron thermal energy. Note that in a HET, thrust is based on $|j_{\theta e}B_r|$ too, but $j_{\theta e}$ is due to the $E \times B$ drift, with E the electric field established between electrodes.

The magnetic nozzle in the HelT is a no-wall device with the consequent advantage of avoiding plasma energy losses and thruster heating. Another virtue is its versatility in shaping the magnetic nozzle through coil tuning. The possible penalty is in thrust efficiency due to large beam divergence caused by plasma/nozzle detachment. The lines of a magnetic nozzle eventually close on themselves and the plasma beam, after completing the supersonic expansion, should detach from them and continue flowing axially. The experimental evidence suggests that the plasma jet detaches, but the physical mechanisms explaining detachment and the efficiency of the process are not well established yet. Theories claiming diffusive detachment via electron diffusion (either resistive or via electron inertia) [93, 94] or via magnetic stretching [95] have been disputed recently [96], at least for the case of a propulsive magnetic nozzle. Instead, detachment would be due to plasma demagnetization, caused by both the divergence of the applied magnetic field and the induced magnetic field created by plasma diamagnetic currents [97, 98].

Magnetic nozzles are not exclusive of the HelT. They are supposed to be the main acceleration stage of the AFMPDT, at least when the self-field is negligible. However, physical processes in the nozzles of AFMPDTs and HelTs might present important differences. In the AFMPDT, the azimuthal electron current has an electromagnetic origin, based on the inter-electrode electric field; the azimuthal ion velocity acquired inside the source can contribute positively and significantly to the thrust [63, 99]; and the internal energy deposited in electrons is possibly smaller. Also, the MPD-arcjet design includes a solid nozzle in addition to the magnetic nozzle; hence, nozzle wall heating is non-zero, although it is expected to be small, because of magnetic screening. The HET with magnetic cusps also bears a magnetic nozzle but its role seems secondary, since the plasma is accelerated before reaching the nozzle region.

Finally, there is the *VASIMR (Variable Specific Impulse Magneto Rocket)*, which consists of a helicon source as the plasma generation stage, a magnetic nozzle as the acceleration stage, and, between them, an ion cyclotron resonance (ICR) antenna as the main heating stage [100, 101]. The ICR antenna imparts gyro-energy to the ions, which is converted into parallel energy in the divergent magnetic nozzle, via the inverse magnetic mirror effect. Since in the VASIMR the internal energy is deposited mainly in ions instead of electrons, we are facing a third variant of magnetic nozzle physics, which would merit a dedicated fluid-dynamical analysis.

The VASIMR, conceived as a megawatt-class thruster, is a rather complex device which, in spite of long-time research (although carried out by a single group almost exclusively), must still prove reliable operation (with all stages active) and its propulsive merits. Among several concerns, the first one is the very large magnetic fields needed to impart enough gyro-energy

to heavy ions. Current tests of the ICR stage with argon apply a peak magnetic field of 2 T [102]. Magnets made of high-temperature superconductors are proposed for creating the required magnetic fields without considerably penalizing the system mass and heat removal. The second concern is whether the matching of helicon and ICR emissions affect plasma heating and thruster operation. Indeed, part of the current research is being carried out with the ICR antenna off, thus the VASIMR is acting as a simple HelT [71].

6. Summary

Plasma thrusters are challenging the monopoly of chemical thrusters in space propulsion by offering much higher specific impulses and, as a consequence, a huge reduction in the propellant mass and the launching cost of a space mission. Plasma thrusters constitute a vast family of devices ranging from already-commercial thrusters to under-development laboratory prototypes. Although many devices can eject a plasma beam and thus produce thrust, a competitive plasma thruster must bear good figures for an ample set of characteristics. Some of the main ones (such as specific impulse, thrust efficiency, lifetime and stable operation) depend specifically on the behavior of the plasma discharge for each particular device.

In this paper, the ion thruster, the HET, the MPDT, the helicon thruster (and some variants of them have been selected in order to illustrate the relevant aspects and issues of the plasma discharge in space thrusters. The IT, the HET and the arcjet constitute the leading group of commercial, mid-power thrusters; the HelT and the AFMPDT could be future members of that group. The rising group of microthrusters is represented by the commercial PPT and near-to-fly electrospray thrusters. Megawatt plasma propulsion, still needing the development of a suitable energy source, is represented by the veteran MPDT and the speculative VASIMR and PIT. Except for the PPT, mature thrusters operate in steady state.

Plasma production is achieved with dc electrodes in the IT, the HET and the MPDT, and with ac radiation in the HelT and alternative ITs; in these last cases, wave energy is deposited either inductively or via different resonances. Plasma acceleration is electrostatic in the IT, electromagnetic in the HET and the MPDT, and electrothermal in the arcjet and the HelT. However, in all cases ion acceleration is mainly electrostatic, driven either by the intergrid space-charge field of the IT or the plasma ambipolar electric field (HET, MPDT and HelT). In electromagnetic devices, the Lorentz force can be based on the applied magnetic field (HET and HelT) or the self-magnetic field (MPDT and PPT); the AFMPT would combine both fields. The applied magnetic field creates a magnetic nozzle in the HelT, the mid-power AFMPDT and the VASIMR. As a solid nozzle, a magnetic nozzle would convert different types of plasma internal or non-axial energy into axial energy, and it would increment thrust. A magnetic nozzle can totally avoid wall heating but efficient plasma detachment must yet be proven.

External magnetic fields are also used in most thrusters to effectively confine the plasma from the chamber walls. Cusped fields created by permanent magnets are a common option. The magnetic topologies of different HET designs exemplify the trade-off between adequately inhibiting the electron axial transport and magnetic screening of the walls. Different crucial processes take place at the plasma–wall interphase. First, there is plasma energy deposition (a direct penalty to thrust efficiency), wall heating and sheath formation. These are affected by magnetic confinement and the wall type (i.e. whether it is an insulator, an isolated metal or an electrode). Second, there is plasma recombination and secondary electron emission (in insulators, SEE can be large and caused by impacting electrons; in thermionic cathodes, SEE is due to heating by ion impact). Third, plasma detachment from the anode has a role in the onset phenomenon of the MPDT and in an unstable operation case of the HET. Fourth, erosion

of the MPDT electrodes, the HET insulating wall and the IT grids are the main limiting factors of the lifetime of these devices, and therefore a subject of unfailing research and improvement.

Except in MPDTs and arcjets, the plasma is weakly collisional and local thermodynamic equilibrium is not ensured. The large SEE from HET insulating walls, the two electron populations in IT chambers or the generation of hot electrons in HelTs are examples of non-Maxwellian electron VDFs. Plasma instabilities and turbulence are also quite ubiquitous and poorly understood generally. Turbulent diffusion in HETs is a prime example since it dominates electron axial transport and heavily affects performances and thrust efficiency. Hydrodynamic and ionization instabilities in HETs cause large discharge oscillations, requiring external filtering for thruster smooth operation. Different instabilities are suggested to have a share in the MPDT onset phenomenon.

As a corollary, space plasma thrusters are being proposed for non-propulsive applications too. The Ion Beam Shepherd (IBS) concept [103] is a spacecraft designed for active removal of space debris, by impinging the plasma plume emitted by an on-board thruster onto a large debris in order to deorbit it; a second plasma thruster provides the compensation force to keep the IBS and the debris at a constant distance. A more adventurous idea (but likely competitive with its peers) is to use the same IBS concept for asteroid deflection [104].

Acknowledgments

This work was supported by the Gobierno de España (Project AYA-2010-16699). The author is very indebted to his colleague and friend Professor Martínez-Sánchez and PhD students M Merino, D Escobar, and R Santos for the many hours spent together trying to clarify the subtleties of plasma discharge phenomena in these space thrusters. The author thanks the referees for their valuable suggestions.

References

[1] Sutton G and Biblarz O 2010 *Rocket Propulsion Elements* (New York: Wiley)
[2] Stuhlinger E 1964 *Ion Propulsion for Space Flight* (New York: McGraw-Hill)
[3] Jahn R 1968 *Physics of Electric Propulsion* (New York: McGraw-Hill) (reprinted by Dover)
[4] Martínez-Sánchez M 2004 *Space Propulsion* Graduate Course available at OpenCourseWare, Massachusetts Institute Technology, http://ocw.mit.edu
[5] Martínez-Sánchez M and Pollard J 1998 *J. Propulsion Power* **14** 688
[6] Jahn R and Choueiri E 2002 Electric propulsion *Encyclopedia of Physical Science and Technology* (New York: Academic) pp 125–41
[7] Brown I 2004 *The Physics and Technology of Ion Sources* (Weinheim, Germany: Wiley-VCH)
[8] Wilbur P 1998 *J. Propulsion Power* **14** 708
[9] Goebel D and Katz I 2008 *Fundamentals of Electric Propulsion: Ion and Hall Thrusters* (New York: Wiley)
[10] Bassner H, Killinger R, Leiter H and Müller J 2001 Development steps of the RF-Ion Thrusters RIT *27th Int. Electric Propulsion Conf. (Pasadena, CA)* IEPC 2001-105 (Fairview Park, OH: Electric Rocket Propulsion Society)
[11] Kuninaka H, Nishiyama K, Funaki I, Shimizu Y, Yamada T and Kawaguchi J 2006 *IEEE Trans. Plasma Sci.* **34** 2125
[12] Lozano P, Sánchez M M and Hubry V 2010 Electrospray propulsion *Encyclopedia of Aerospace Engineering* (New York: Wiley Online Library)
[13] Marcuccio S, Genovese A and Andrenucci M 1998 *J. Propulsion Power* **14** 774
[14] Kim V 1998 *J. Propulsion Power* **14** 736
[15] Zhurin V, Kaufman H and Robinson R 1999 *Plasma Sources Sci. Technol.* **8** R1
[16] Ahedo E, Gallardo J and Martínez-Sánchez M 2003 *Phys. Plasmas* **10** 3397
[17] Ahedo E and Escobar D 2004 *J. Appl. Phys.* **96** 983

[18] Barral S, Makowski K, Peradzynski Z, Gascon N and Dudeck M 2003 *Phys. Plasmas* **10** 4137
[19] Fife J M 1998 Hybrid-PIC modeling and electrostatic probe survey of Hall thrusters *PhD Thesis* Massachusetts Institute of Technology
[20] Parra F, Ahedo E, Fife M and Martínez-Sánchez M 2006 *J. Appl. Phys.* **100** 023304
[21] Hagelaar G, Bareilles J, Garrigues L and Boeuf J 2002 *J. Appl. Phys.* **91** 5592
[22] Szabo J J 2001 Fully kinetic numerical modeling of a plasma thruster *PhD Thesis* Massachusetts Institute of Technology
[23] Adam J C, Herón A and Laval G 2004 *Phys. Plasmas* **11** 295
[24] Mikellides I, Katz I, Hofer R, Goebel D, de Grys K and Mathers A 2011 *Phys. Plasmas* **18** 033501
[25] Harrison E and Thompson W 1959 *Proc. Phys. Soc. London* **74** 145
[26] Ahedo E, Santos R and Parra F 2010 *Phys. Plasmas* **17** 073507
[27] Hobbs G and Wesson J 1967 *Plasma Phys.* **9** 85
[28] Ahedo E 2002 *Phys. Plasmas* **9** 4340
[29] Ahedo E and de Pablo V 2007 *Phys. Plasmas* **14** 083501
[30] Kaganovich I D, Raitses Y, Sydorenko D and Smolyakov A 2007 *Phys. Plasmas* **14** 057104
[31] Ahedo E and Parra F 2005 *Phys. Plasmas* **12** 073503
[32] Ahedo E, Antón A, Garmendia I, Caro I and del Amo J G 2007 Simulation of wall erosion in Hall thrusters *30th Int. Electric Propulsion Conf. (Florence, Italy)* (Fairview Park, OH: Electric Rocket Propulsion Society) IEPC 2007-067
[33] Garnier Y, Viel V, Roussel J-F and Bernard J 1999 *J. Vac. Sci. Technol.* A **17** 3246
[34] Morozov A and Savelyev V 2000 Fundamentals of stationary plasma thruster theory *Reviews of Plasma Physics* Vol 21 (New York: Kluwer)
[35] Janes G and Lowder R 1966 *Phys. Fluids* **9** 1115
[36] Morozov A, Esipchuk Y, Tilinin G, Trofimov A, Sharov Y and Shchepkin G Y 1972 *Sov. Phys.-Tech. Phys.* **17** 38
[37] Bugrova A, Morozov A and Kharchevnikov V K 1990 *Sov. J. Plasma Phys.* **16** 849
[38] Garrigues L, Hagelaar G, Boniface C and Boeuf J 2006 *J. Appl. Phys.* **100** 123301
[39] Choueiri E 2001 *Phys. Plasmas* **8** 1411
[40] Barral S, Makowski K, Peradzynski Z and Dudeck M 2005 *Phys. Plasmas* **12** 073504
[41] Barral S and Ahedo E 2009 *Phys. Rev.* E **79** 046401
[42] Parker J, Raitses Y and Fisch N 2010 *Appl. Phys. Lett.* **97** 091501
[43] Lazurenko A, Krasnoselskikh V and Bouchoule A 2008 *IEEE Trans. Plasma Sci.* **36** 1977
[44] Terry P W 2000 *Rev. Modern Phys.* **72** 109
[45] Khayms V and Martínez-Sánchez M 2000 Fifty-watt Hall thruster for microsatellites *Micropropulsion for Small Spacecraft, Progress in Astronautics and Aeronautics* vol 187 (Washington, DC: American Institute of Aeronautics and Astronautics)
[46] Ahedo E and Gallardo J 2003 Scaling down Hall thrusters *28th Int. Electric Propulsion Conf. (Toulouse, France)* (Fairview Park, OH: Electric Rocket Propulsion Society) IEPC 2003-104
[47] Raitses Y and Fisch N 2001 *Phys. Plasmas* **8** 2579
[48] Warner N 2007 Theoretical and experimental investigation of Hall thruster miniaturization *PhD Thesis* Massachusetts Institute of Technology
[49] Kaufman H 1985 *AIAA J.* **23** 78
[50] Ahedo E and Parra F 2005 *J. Appl. Phys.* **98** 023303
[51] Escobar D and Ahedo E 2008 *IEEE Trans. Plasma Sci.* **36** 2043
[52] Kornfeld G, Koch N and Harmann H 2007 Physics and evolution of HEMP-thrusters *30th Int. Electric Propulsion Conf. (Firenze, Italy)* (Fairview Park, OH: Electric Rocket Propulsion Society) IEPC 2007-108
[53] Courtney D and Martínez-Sánchez M 2007 Diverging cusped-field Hall thruster *30th Int. Electric Propulsion Conf. (Florence, Italy)* (Fairview Park, OH: Electric Rocket Propulsion Society) IEPC 2007-39
[54] Martínez-Sánchez M and Ahedo E 2011 *Phys. Plasmas* **18** 033509
[55] Choueiri E 1998 *J. Propulsion Power* **14** 744
[56] Andrenucci M 2010 Magnetoplasmadynamic thrusters *Encyclopedia of Aerospace Engineering* (New York: Wiley Online Library)
[57] Martinez-Sanchez M 1991 *J. Propulsion Power* **7** 56
[58] Baksht F, Moizhes B and Rybakov A 1974 *Sov. Phys. Tech. Phys.* **18** 1613
[59] Ahedo E and Rus J 2005 *J. Appl. Phys.* **98** 043306
[60] Kodys A and Choueiri E 2005 A critical review of the state-of-the-art in the performance of applied-field magnetoplasmadynamic thrusters *41st AIAA Joint Propulsion Conf. (Tucson, AZ)* (Washington, DC: American Institute of Aeronautics and Astronautics) AIAA 2005-4247

[61] Toki K, Shimuzu Y and Kuriki K 1997 Electric propulsion experiment (EPEX) of a repetitively pulsed MPD thruster syslem onboard Space Flyer Unit (SFU) *25th Int. Electric Propulsion Conf. (Cleveland, OH)* (Fairview Park, OH: Electric Rocket Propulsion Society, Fairview) IEPC 97-120
[62] Krülle G, Auweter-Kurtz M and Sasoh A 1998 *J. Propulsion Power* **14** 754
[63] Fradkin D, Blackstock A, Roehling D, Stratton T, Williams M and Liewer K 1970 *AIAA J.* **8** 886
[64] Lovberg R H and Dailey C L 1982 *AIAA J.* **20** 971
[65] Burton R and Turchi P 1998 *J. Propulsion Power* **14** 716
[66] Chen F 1995 *Phys. Plasmas* **2** 2164
[67] Ziemba T, Carscadden J, Slough J, Prager J and Winglee R 2005 High power helicon thruster *41th Joint Propulsion Conf. (Tucson, AR)* (Washington, DC: American Institute of Aeronautics and Astronautics) AIAA 2005-4119
[68] West M, Charles C and Boswell R 2008 *J. Propulsion Power* **24** 134
[69] Batishchev O 2009 *IEEE Trans. Plasma Sci.* **37** 1563
[70] Pavarin D *et al* 2011 Thruster development set-up for the helicon plasma hydrazine combined micro research project *32th Int. Electric Propulsion Conf. (Wiesbaden, Germany)* (Fairview Park, OH: Electric Rocket Propulsion Society) IEPC 2011-241
[71] Longmier B *et al* 2011 *Plasma Sources Sci. Technol.* **20** 015007
[72] Chen F 1991 *Plasma Phys. Control. Fusion* **33** 339
[73] Boswell R 1984 *Plasma Phys. Control. Fusion* **26** 1147
[74] Shamrai K and Taranov V 1994 *Plasma Phys. Control. Fusion* **36** 1719
[75] Chen F 1996 *Phys. Plasmas* **3** 1783
[76] Ahedo E 2009 Cylindrical model of a helicon-generated plasma *31st Int. Electric Propulsion Conf. (Ann Arbor, Michigan)* (Fairview Park, OH: Electric Rocket Propulsion Society) IEPC 2009-193
[77] Arefiev A and Breizman B 2006 *Phys. Plasmas* **13** 062107
[78] Chen T R S and Hershkowitz N 1998 *Phys. Rev. Lett.* **80** 4677
[79] Scharer J, Degeling A, Borg G and Boswell R 2002 *Phys. Plasmas* **9** 3734
[80] Cohen S A, Sun X, Ferraro N, Scime E E, Miah M, Stange S, Siefert N and Boivin R 2006 *IEEE Trans. Plasma Sci.* **34** 792
[81] Bezzerides B, Forslund D W and Lindman E L 1978 *Phys. Fluids* **21** 2179
[82] Hairapetian G and Stenzel R L 1991 *Phys. Fluids* B **3** 899
[83] Charles C and Boswell R 2003 *Appl. Phys. Lett.* **82** 1356
[84] Ahedo E and Martínez-Sánchez M 2009 *Phys. Rev. Lett.* **103** 135002
[85] Charles C, Boswell R and Lieberman M 2006 *Appl. Phys. Lett.* **89** 261503
[86] Raadu M A 1989 *Phys. Rep.* **178** 25
[87] Fruchtman A 2006 *Phys. Rev. Lett.* **96** 065002
[88] Ahedo E 2011 *Phys. Plasmas* **18** 033510
[89] Ahedo E 2009 *Phys. Plasmas* **16** 113503
[90] Freidberg J 2007 *Plasma Physics and Fusion Energy* (Cambridge: Cambridge University Press)
[91] Tysk S, Denning C, Scharer J and Akhtar K 2004 *Phys. Plasmas* **11** 878
[92] Ahedo E and Merino M 2010 *Phys. Plasmas* **17** 073501
[93] Moses R W, Gerwin R and Schoenberg K 1992 Resistive plasma detachment in nozzle based coaxial thrusters *9th Symp. on Space Nuclear Power Systems (Albuquerque, New Mexico, 1992)* (Woodbury, NY: American Institute of Physics) *AIP Conf. Proc.* **246** 1293–303
[94] Hooper E B 1993 *J. Propulsion Power* **9** 757
[95] Arefiev A and Breizman B 2005 *Phys. Plasmas* **12** 043504
[96] Ahedo E and Merino M 2011 *Phys. Plasmas* **18** 053504
[97] Merino M and Ahedo E 2010 Plasma detachment mechanisms in a magnetic nozzle *47th Joint Propulsion Conf. (San Diego, CA)* (Washington, DC: American Institute of Aeronautics and Astronautics) AIAA 2011-5999
[98] Roberson B, Winglee R and Prager J 2011 *Phys. Plasmas* **18** 053505
[99] Sasoh A 1994 *Phys. Plasmas* **1** 464
[100] Diaz C 2000 *Sci. Am.* **283** 90
[101] Arefiev A and Breizman B 2004 *Phys. Plasmas* **11** 2942
[102] Longmier B *et al* 2011 *J. Propulsion Power* **27** 915
[103] Bombardelli C and Peláez J 2011 *J. Guid. Control Dyn.* **34** 916
[104] Bombardelli C, Peláez J, Ahedo E, Urrutxua H and Merino M 2011 The ion beam shepherd, a new concept for asteroid deflection, Presented at *2011 IAA Planetary Defense Conf. (Bucharest, Romania, 09–12 May 2011)*